CARBONATION EVOLUTION OF LIME PUTTY COATINGS WITH MUSSEL SHELL AGGREGATE

Abstract

The carbonation process is studied from young ages up to 2 years in mortars with fine mussel shell aggregate. Mussel shell aggregate affects lime mortars due to its shape (angular and flaky) and texture (smooth), and also its microstructure consisting of 2% organic matter in the form of protein and polysaccharides (chitin). Its affect is analysed in pore structure, microstructure by SEM, carbonation by phenolphthalein, and mechanical strength by means of compressive strength and ultrasounds. Conclusions show that the use of mussel shell aggregate delays carbonation at young ages while increasing the total carbonated area at old ages. These two different trends can be seen in all of the properties analysed.

Keywords:

Air lime; porosity; pore size distribution; compressive strength; ultrasounds; ageing

Highlights:

- The density increase rate due to carbonation is higher in mussel mortars
- The organic matter content modifies the microstructure of CaCO3 polymorphs
- Mussel organic matter promotes water retention in lime mortars
- Mussel shell slows down carbonation at young ages, but promotes it at older ages
- Porosity and ITZ of mussel shell mortars significantly affect mechanical performance

1 Introduction and objectives

In this work, the carbonation process of lime putty mortars is analysed. This process hardens air lime mortars and involves the redistribution of pore size. It consists of an increase in the solid volume of the paste caused by the transformation of calcium hydroxide into calcium carbonate. Carbonation affects every property of air lime mortars.

It is well known that there are several factors that affect carbonation in air lime mortars: water to lime ratio, type of lime, ageing of lime, curing conditions and aggregate. Aggregates have a very important influence on the carbonation of air lime mortars. The differences found among the characteristics, mineralogy, grading and shape of aggregates used in mortars are factors that can influence carbonation and hence the behaviour of the final coating. All of these aggregate parameters can influence the mortar's microstructure and define a specific porous matrix. The pore structure of mortars is what ultimately outlines the behaviour in both the drying and carbonation process, promoting the transport of water and ions.

The mineralogical nature of aggregates along with their particle size distribution are important issues for good lime mortar performance [1]. To ensure the best compactness and hence good behaviour and durability, sand should be well graded with a large range of grain size and mineralogy which favours good connection with the lime. [2] These are important issues for achieving good behaviour and durability.

In general, in mortars the use of different sand sources other than the conventional affects flow ability, strength and toughness [3]. It was also studied that angular shaped aggregates increase the water demand in cement mortars, while the ITZ in such cases improves even though the porosity increases [4]. In lime mortars, the use of fine recycled sand [5], originating from mixed construction and demolition waste was studied.

The replacement in lime mortars of conventional aggregate with mussel shell sand was studied in an earlier work[6]. In lime mortar, mussel shell sand particles not only have an affect as an aggregate

(grading, shape, texture, fineness, etc.) due to their microstructure, but also as an additive due to the organic matter content.

It is known that the use of additives, both mineral (pozzolans [7] , nanosilica [8], fillers [9], etc.) and organic (water retention [10] , water-repellent agents [11], air-entraining agent[12], organic fibres [13], etc.) induce changes in the characteristics and affect both the performance and durability of lime mortars. Additives should be taken into account in the carbonation reaction in lime mortars. Natural additives with organic content were used in ancient coatings. As studied by other authors, organic additives could be used to enhance different properties of lime mortars and have a significant impact on the carbonation process due to their protein, fatty acid and/or polysaccharide content. In different works [14–16], it was discovered that fatty acids, compounds of different oils (olive, linseed, spent cooking oils) added to lime mortar mixes can delay or decelerate the carbonation rate. However, the polysaccharides mainly present in different additives like nopal (powder and mucilage) [14], Areca nut extract [17] and brown sugar (disaccharides)[18] are responsible for an increase in the carbonation rate of air lime mortars. Protein, also has the same impact on mortars, as seen in works that used sticky rice or pigs blood [19] and albumen [16]. Although, there is a study that analysed the use of oxblood [20] as an additive which concludes that this protein slows down the carbonation rate at younger ages, at 1 year of age it was observed that the mortar produced similar amounts of carbonates to the specimens without the additive. However, a reduction in the carbonation rate was observed when protein and albumen [16] were used together.

In a previous work [6], the carbonation degree of mussel shell mortars was evaluated at the age of one year for two different binders: lime putty and hydrated lime. In lime putty mortars, at this age, carbonation increases significantly with the increase of mussel shell content. However, mechanical strength and ultrasonic wave propagation decreases in mussel shell mortars, caused by the higher porosity and a lack of bond between mussel shell particles and the air lime paste.

As it is well known that lime mortars can take many years to reach total carbonation, in this study the properties were evaluated from young ages up to 2 years from the preparation of the batches. The study

of the development of this hardening process in air lime mortars with mussel shell aggregate may contribute to understanding the long-term behaviour of lime coatings, and predict their stability over time.

2 Materials and mixes

The binder used in this study was a slaked lime putty (PL) with a water content by weight of 64% (EN 459-1 CL90-PL) and a storage age of 10 months. The composition by XRF and TGA results were already published in a previous work [6].

Two types of aggregates were used, limestone sand (LS) and mussel shell sand (MS). A suitable size separation and combination of the LS was performed resulting in a sand with a maximum size of 2 mm (LS) and a fineness modulus of 2.23. The mussel shell sand used was obtained from mussel shells after heat treatment in a trommel rotary screen at 135°C for 32 minutes. After crushing and sieving two fractions were obtained: a coarse sand (CMS 0-4mm) and a fine sand (FMS 0-1mm). These two fractions were combined to obtain the MS with a fineness modulus equivalent to that of LS (2.21). The water absorption (UNE-EN 1097-6) of the LS is 2.22%.

Mussel shells are divided into three parts: the outer layer or periostracum, the middle layer called the prismatic layer and the inner layer referred to as nacre. The microstructure of the mussel shell particle was detailed in a previous work [21]. The central and thickest layer has a prismatic structure with an array of parallel calcite prisms. Both external and internal layers have organic matter content consisting of polysaccharides (chitin), proteins and glycoproteins [22]. This organic matter content is present at 2.1% in the combined mussel shell sand. The water absorption of MS is 3.9%. A more detailed characterisation of binder and aggregates has already been published in a previous work [6].

A baseline mortar PL0 was designed with a binder to aggregate ratio of 1:2.5 (by volume). MS mortars were obtained replacing LS with MS at the following substitution rates 25%, 50% and 75% (PL25, PL50, and PL75). For the dosages, 629.1 g of lime putty was used for each mortar. PL0 used 1270.3 g of LS, PL0

used 952.7 g of LS and 323.52 g of MS, PL50 used 635.1 g of LS and 674.0 g of MS, and finally PL75 used 317.6 g of LS and 970.6

Mortars were mixed according to UNE-EN 196-1 and were cast according to UNE-EN 1015-11 in prismatic moulds (40x40x160 mm) for density, carbonation and mechanical strength testing. In addition, cylindrical PVC tubes of 150 mm diameter and 20 mm thickness were made for porosity tests. A manual compaction system with a 50 g rammer was used to remove air bubbles. Moulds were placed in the climatic chamber (20 °C ± 2 and 60 ± 5%) for 5 days before demoulding. The CO_2 concentration in the chamber was estimated to be the standard atmospheric concentration (i.e. 0.033 ± 0.001% by volume). All tests were carried out at different ages, from fresh state up to 1 or 2 years of age.

3 Test methods

3.1 Density, compressive strength, ultrasonic wave propagation and carbonation

Hardened density was calculated using prismatic specimens of 160x40x40 mm over at least tree samples. Density values were registered from fresh state up to 2 years.

Ultrasonic measurement equipment, Pundit Lab from Proceq, was used to perform the ultrasonic test in transmission reception mode. The frequency of both transducer couples was 150 Hz. Two measurements were made on each prismatic specimen, both parallel and perpendicular to the cast direction. Three specimens were used for each mortar, thus six speeds were registered. The ultrasound velocity was measured at 7, 28, 180 days and 1 and 2 years age.

Then, the compressive strength test was carried out according to UNE EN 1015-11 on three prismatic specimens using a universal compression/flexural machine. The test velocity selected for compressive strength tests was 0.15 kN/s. The compressive strength was measured at 7, 28, 90, 180 days and 1 and 2 years of age.

Carbonation over time was observed by impregnating the mortar samples with a saturated phenolphthalein ethyl alcohol solution. Three test samples of each mortar were tested. Each prismatic

sample was broken (flexural test) and tested with phenolphthalein solution at 28, 56, 90, 180 days and 1 and 2 years of age.

3.2 Porosity, pore size distribution and texture characterisation

By means of a core-drill, at least three pieces were taken from different cylindrical samples of hardened lime mortars at the ages of 28 days, 120 days and 1 year. They were used to measure accessible porosity for water according to UNE 83980. After this test, open porosity values after water immersion, and after water immersion and boiling were obtained.

In addition, the pore size distribution analysis was performed with a Mercury Intrusion Porosimetry (MIP), which automatically registers pressure, pore diameter in a range between 0.003 to 200 μm, intrusion volume, and pore surface area. The range of pressure used was 6.29 kPa to 410759.65 kPa.

Different specimens were examined and photographed under a scanning electron microscopy (SEM).

4 Results and discussion.

4.1 Density

Density evolution of the lime mortars is shown in Figure 1. First, a weight decrease is observed due to the water loss, until the specimens reach equilibrium with the moisture of the environment. Then, the densification of the samples (increase in weight) is measured from 28 days on. This increase in weight is caused by the carbonation process that produces a decrease in porosity, resulting in an increase in compactness [23].

In all cases, density is lower with the mussel content, due to the introduction of air caused by the particle shape and organic matter content of the mussel aggregate, as observed in previous works [6,24]. It is also notable, that the increase in weight is faster in mussel shell mortars than the baseline mortars. This is related to the carbonation rate as discussed in section 4.4.

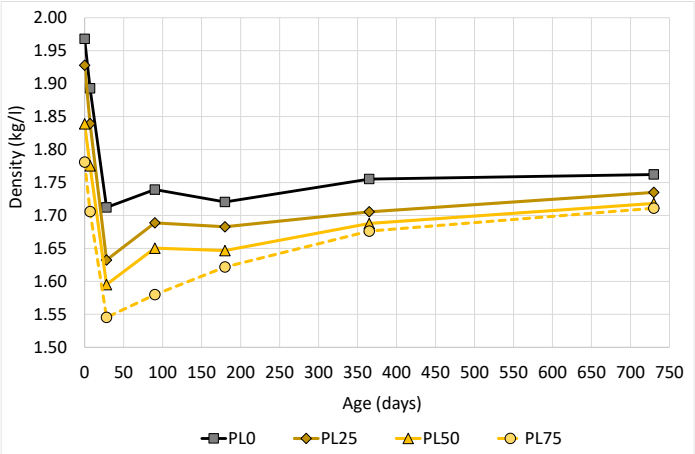

Figure 1. Density evolution from fresh state to 2 years of age.

4.2 Pore structure

Pore size distribution and total porosity were measured at four different ages from 28 days up to 2 years of age. Total porosity was measured by three different methods: water absorption after immersion (P-AI), water absorption after immersion and boiling (P-AIB) according to UNE 83980 and lastly by mercury intrusion (P-MIP), Figure 2.

Porosity results of PL75 samples at 28 days (measured by water absorption after immersion and after immersion and boiling) are not shown in the graph because they were considered invalid as a consequence of material loss suffered in the test. This is caused by the poor binding ability of the matrix with a low carbonation degree at this age, the lack of bond between mussel shell particles and lime paste [6,21,24] and the high porosity of the samples.

P-AIB shows higher values than P-AI, especially in mussel shell mortars with a high replacement content. This is because the pressure of boiling water allows water to reach more pores than the simple absorption after immersion test. Mussel shell acts as a barrier to water penetration which can be overcome by boiling the water.

Porosity measured by MIP should show the highest porosity values of the three methods, however it shows a different trend with high mussel shell content, with PA-AIB higher than P-MIP. This is explained

by the limitation of the range of measurement of MIP, which does not account for pores larger than 200 µm. Mussel shell mortars show a high volume of these large pores that cannot be measured with P-MIP.

As seen in Figure 2, porosity is higher in mussel shell mortars than the baseline mortar at all ages due to the higher volume of air voids introduced by the mussel shell particles. PL0 and PL25 showed similar porosity values at all ages, especially when measured by water absorption after immersion.

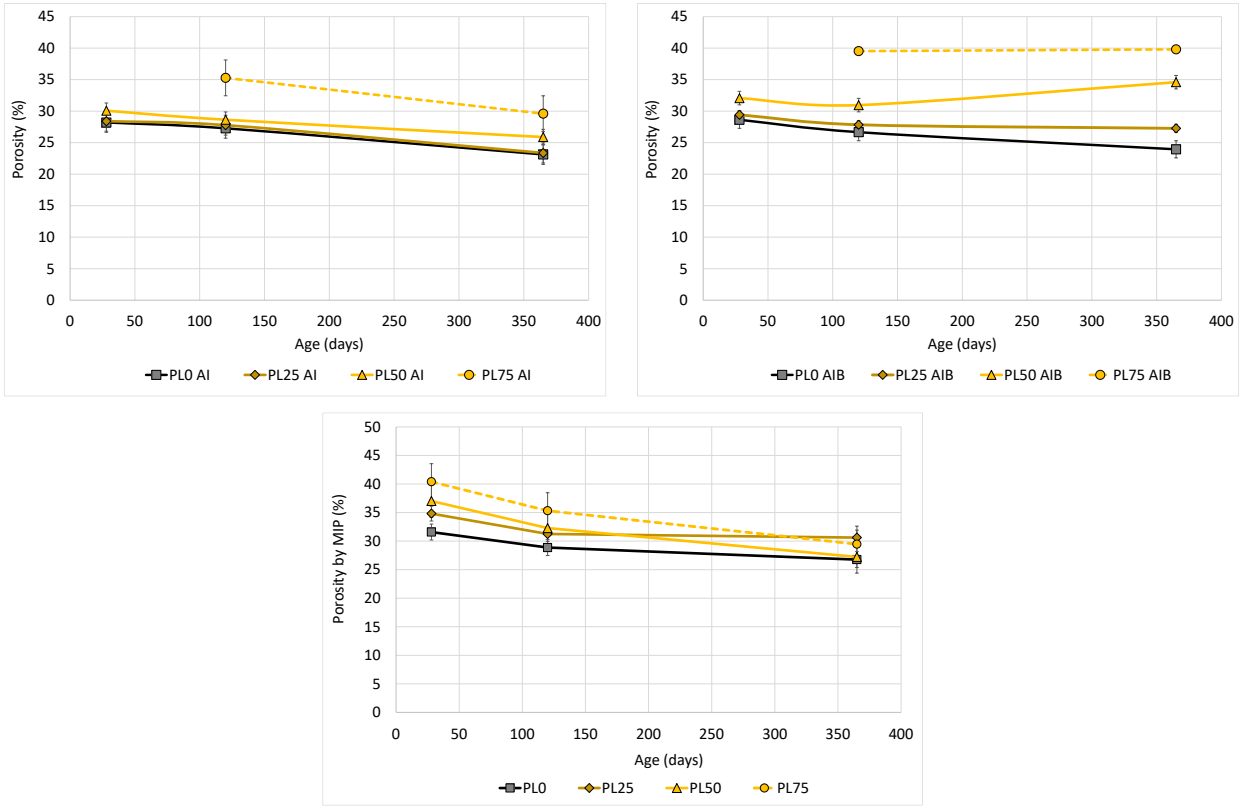

Figure 2. Porosity measured by water absorption after immersion (AI), water absorption after immersion and boiling (AIB), and mercury intrusion (MIP).

In general, the porosity evolution shows a decline over time, that is expectable due to the carbonation process and is consistent with the density results. In Figure 3 it can be seen that densities increase while porosities (by MIP) decrease with age. This trend is similar in all mortars, although mussel mortars with a high replacement rate (50% and 75%) show higher changes in density and porosity with age than 0% and 25% mortars.

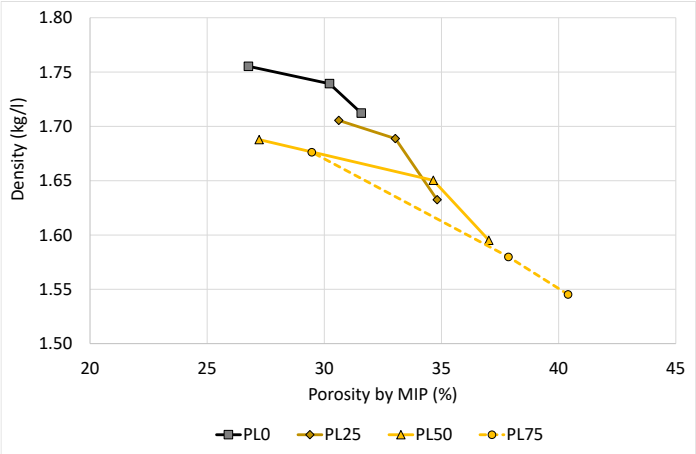

Figure 3. MIP values vs. densities.

Pore size distribution of lime putty mortars at 28 days, 120 days and 1 year are shown in Figure 4. As stated in a previous work [6] lime mortars show a bimodal distribution with two peaks: structural peak (composed by pores with a diameter between 0.1 and 1 µm) and a second peak (ITZ peak), that corresponds with the pores in the interfacial transition zone (consisting of pores between 5 and 30 µm). Figure 5 shows the evolution of both main peaks of all mortars over time.

The peak at around 1.0 µm is not seen as a change in pore structure in the mortars. This pore size is fixed in the binder on drying and depends on the water to lime ratio [25]. All mortars were designed with the same water to lime ratio, and hence are expected to show a similar structural peak, although mussel shell mortars present lower values at this peak for all ages (Figure 5). The higher absorption of mussel shell aggregate (3.9%) in comparison to limestone sand (2.2%), and the fact that mussel shell aggregate could act as a moisture retainer due to the barrier effect of the flaky particles [6], reduces the mixing water enabled to evaporate, thereby generating less pore volume at this peak.

However, the ITZ peak is clearly different in conventional mortar when compared to mussel shell mortars. As seen in previous works [6], the bond between paste and mussel aggregate is weak and a high amount of pores can be seen in the mussel aggregate ITZ mortars. Therefore, the volume and size of pores of the second peak is considerably higher in mussel mortars than in conventional mortar (Figure

4 and Figure 5), especially when a high replacement percentage of mussel aggregate is used. Furthermore, the plotted graph shows that the range of this peak is wider in mortars with high mussel content. It is also notable that this wide range gets narrower over time (Figure 4).

Analysing the two main peak ranges over time (Figure 5), it can be seen that in reference mortars the reduction due to carbonation is almost the same at both peaks, and is around 15% from 28 days to 1 year of age. However, mussel shell mortars show a higher porosity reduction than the reference mortar which is different at each peak (Figure 4). Variations observed in the structural peak are around 15% in PL25 and PL50, but are close to 30% in PL75 at 1 year of age. Variations in the ITZ peak are significantly higher than in the structural peak, being 22%, 28% and 40% for PL25, PL50 and PL75 respectively. This is due to the higher carbonation rate observed when mussel aggregates are used (see section 4.4). Therefore, the calcium carbonate crystals are attaching themselves to the aggregate particles and, in doing so, reducing the size and volume of the pores at the interface between the mussel aggregate and the calcite.

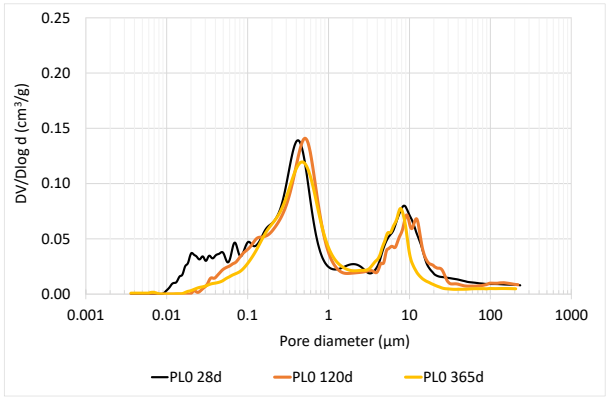

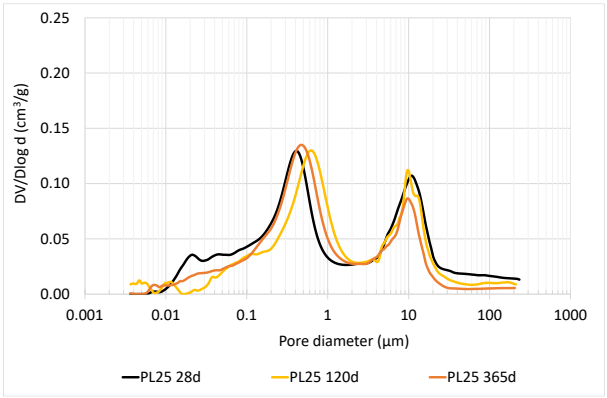

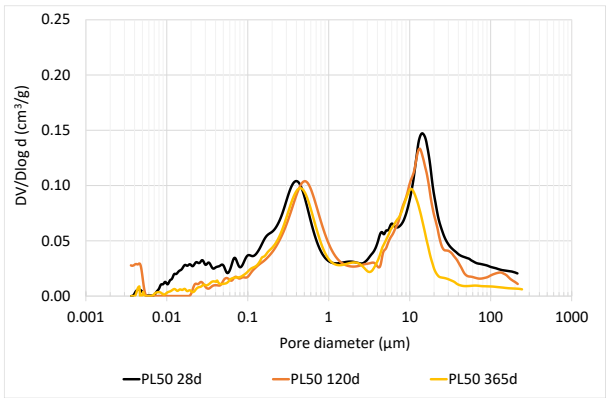

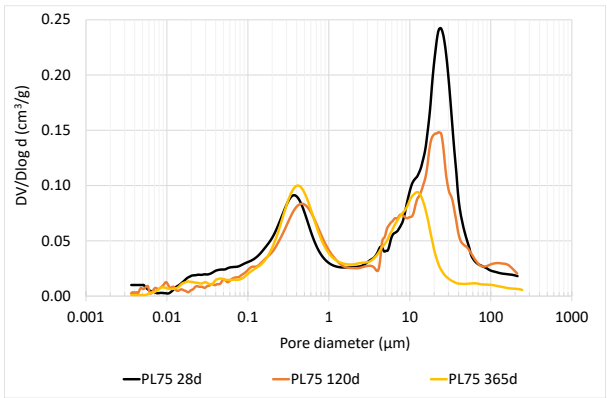

Figure 4. Pore size distribution at 28, 120 days and 1 year of age.

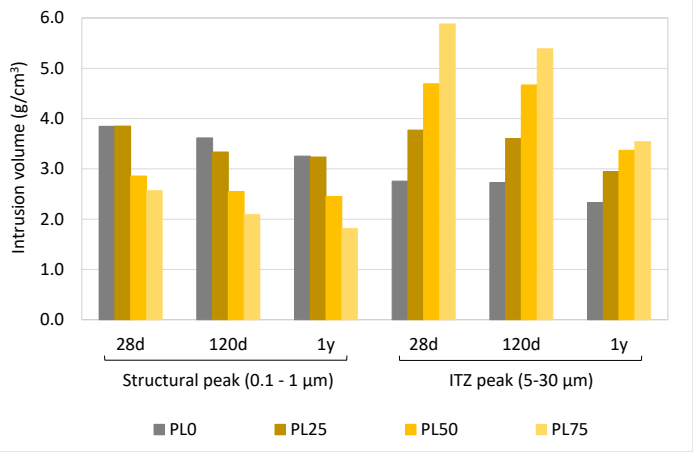

Figure 5. Pore range of the two main peaks of each mortar at different ages.

4.3 Microstructure

As already studied, in the initial stages of carbonation, precipitated spherulitic CaCO3 can be found on the basal faces of portlandite crystals, which is associated with the formation of amorphous calcium carbonate (ACC). When carbonation evolves, calcite grows as micro-meter sized scalenohedral crystals followed by a transformation to rhombohedral form upon exposure to high CO2 concentration [26–28]. Cizer et al. [26] discovered that calcite crystals displayed different habits and morphology through the sample thickness due to the CO2 concentration and environmental conditions (humidity). Apart from this, organic matter content can disturb the morphology and growth of calcium carbonate and their polymorphs [29].

SEM images of the baseline mortar (PL0) and the highest mussel shell replacement rate (PL75) at 28, 120 and 365 days are shown in Figure 6 and Figure 7. The images clearly show different morphologies of the calcite microstructure between the reference and mussel shell matrix.

In Figure 6 it can be seen that carbonation leads to the densification of both mortars' microstructure over time and changes in the morphology of the crystals. In PL75 it is observed that paste is more disaggregated at all ages when compared to the reference sample. Also, a lack of bond between mussel

shell particles and lime paste can be seen at 28 days. Furthermore, at 1 year of age some small drying cracks are observed.

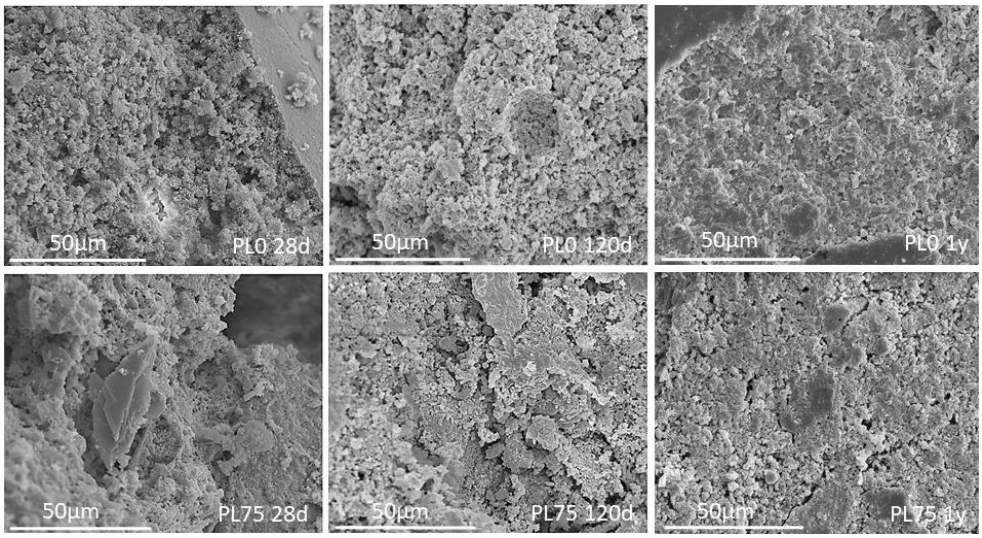

Figure 6. SEM images (1000x) at 28, 120 and 365 days of PL0 and PL75.

In Figure 7 differences in the crystallisation of calcium carbonate between PL75 and PL0 can be analysed. At 28 days, in reference mortar, plate like portlandite crystals are observed, many of which displaying precipitated ACC on the basal surfaces. At 120 days, these amorphous calcite crystals (spherical shape) are transformed into rosette shape scalenohedral calcite, as already observed in similar mortars by other authors [12,30]. Although scalenohedral form is the most abundant morphology in the 120-day-sample, plate-like portlandite, with spherulitic morphology growing on them, is also observed. This means that carbonation is still incomplete. At 1 year of age PL0 shows an important increase in density and the crystals are more uniform, displaying a highly compact structure. Furthermore, at this age, rhombohedral morphology is the main crystal shape observed. It can clearly be seen that the pores surrounding the crystals are getting smaller over time.

In mussel shell mortar (PL75) crystallisation of calcium carbonate is notably different. In general, chaotic distribution of crystals is the main characteristic observed at all ages. At 28 days, plate-like portlandite crystals are hardly seen and the calcite crystals seem to be smaller in comparison to the reference mortar. The morphology of these calcite crystals shows spherical shapes heaped on top of each other,

typical of vaterite morphology, a metastable calcium carbonate polymorph related to a slower growth rate [31]. It is observed that there are some large column shaped crystals of calcite belonging to the prismatic layer of the mussel shell particle. These appear isolated and broken at 28 and 120 days, and hardly adhered to the lime paste. Some acicular crystals of aragonite are detected in mussel shell samples, again at 28 and 120 days. Metastable $CaCO_3$ polymorph, as aragonite and vaterite, are also seen by Ventolá et al. [14] when organic additives are used in the preparation of mortars. At one year of age, the PL75 sample presents calcite crystals with a rounded morphology and smaller grain size when compared to the same crystals in the reference mortar, again due to the presence of organic compounds. This was also observed by Zhao et al. when sticky rice, Tung oil and pigs blood were used as additives [19]. This also agrees with the results of Gour et al. [17] that observed how organic matter content modifies the texture and microstructure of calcite and vaterite polymorphs.

In SEM images the presence of halite (NaCl) crystals is also observed (Figure 7), but only at early ages in all the mussel shell samples, being negligible at 1 year of age. As it is known, lime mortars are prone to salt crystallisation in the pores (crypto-florescence) due to their bimodal pore distribution and low mechanical strength [32]. This crystallisation results in pressure against the pore wall producing significant deterioration (cracking, crumbling, etc.) of the mortars. This phenomenon usually occurs on the already hardened material, due to substrate typology or environmental conditions when salts are derived from masonry materials or provided from exterior sources (salt laden wind, salt from soils through rising damp, etc.)[33]. However, there is a lack of information about the effect that sodium chloride has on lime mortars when in the kneading water, as is the case when using marine aggregates. Although this phenomenon needs further research, it is probable that sodium chloride reacts with calcium hydroxide, giving us an expansive reaction that produces sodium carbonate and calcium chloride. This expansive reaction could be responsible for the cracks that are visible in the paste in mussel shell mortars (Figure 6).

It can be concluded, that mussel shell content changes the morphology evolution of calcium carbonate crystals, thereby affecting the carbonation process as seen in the following section.

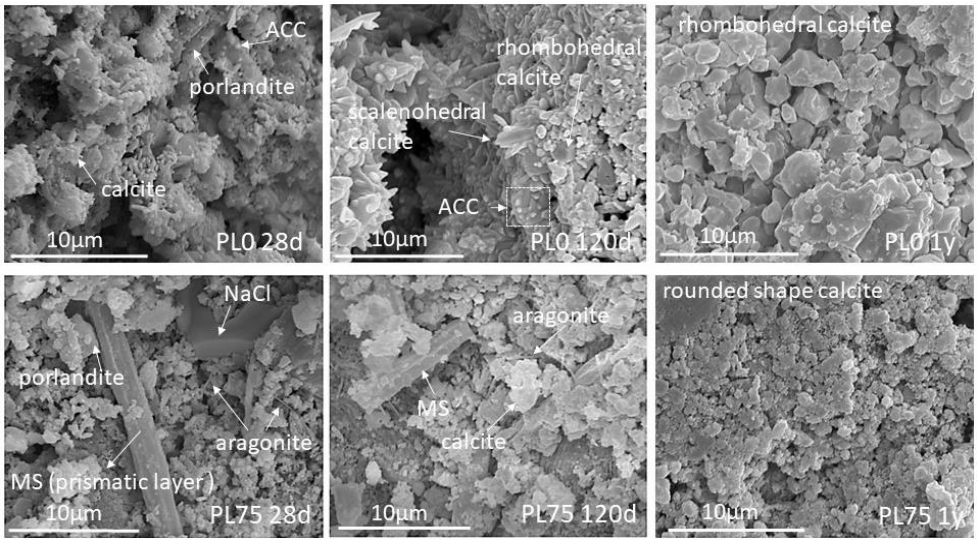

Figure 7. SEM images (5000x) at 28, 120 and 365 days of PL0 and PL75.

4.4 Carbonation

The rate of carbonation from 28 days to 2 years of age measured by the phenolphthalein method is shown in Figure 8. Figure 9 shows the average value of the carbonated surface area obtained with three samples of each mortar.

It can be stated that the carbonation rate in lime mortars with mussel shell used as an aggregate presents two different trends. At young ages it is observed that mussel shell reduces carbonation. However, from 180 days onward this trend changes and then the greater the mussel shell content the greater the carbonated area observed. At one year PL50 and PL75 show a 10% and 20% higher carbonation degree (respectively) than PL0, and at two years PL75 is completely carbonated while PL0 is not.

This can be explained by pore structure, flaky mussel particles and organic matter content.

The water exchange capacity of mussel shell mortars is low. The rate of liquid water transport within mussel shell mortars is hampered by the blockage effect and ability to retain moisture, caused by flaky mussel particles and the organic matter content [17]. Therefore, the mussel particle shape and its

organic matter content delay the drying process necessary to initiate carbonation. Hence, at early ages the carbonation rate of mussel mortars is lower than that of conventional mortar.

At older ages, however, two different phenomenon promote carbonation in mussel mortars. Firstly, their high volume of large pores. It is well-known that large pores have a major contribution to carbonation. The high volume of pores larger than 10 µm, offers great access to the diffusion of atmospheric CO_2 [34] in the mortar. Furthermore, the aforementioned blockage leaves more available water inside mussel shell mortars than in the reference mortar. As stated by Gour et al. [17], the polysaccharides help to retain moisture which promotes the dissolution of reactants and allows carbonation to develop significantly. This justifies the change in the carbonation rate observed at 180 days old, and finally leads mussel mortars to present a higher carbonation rate than reference mortars at 1 and 2 years of age. This also agrees with some ancient practices carried out by traditional craftsmen, who dampened and dried lime mortar to improve its carbonation [35].

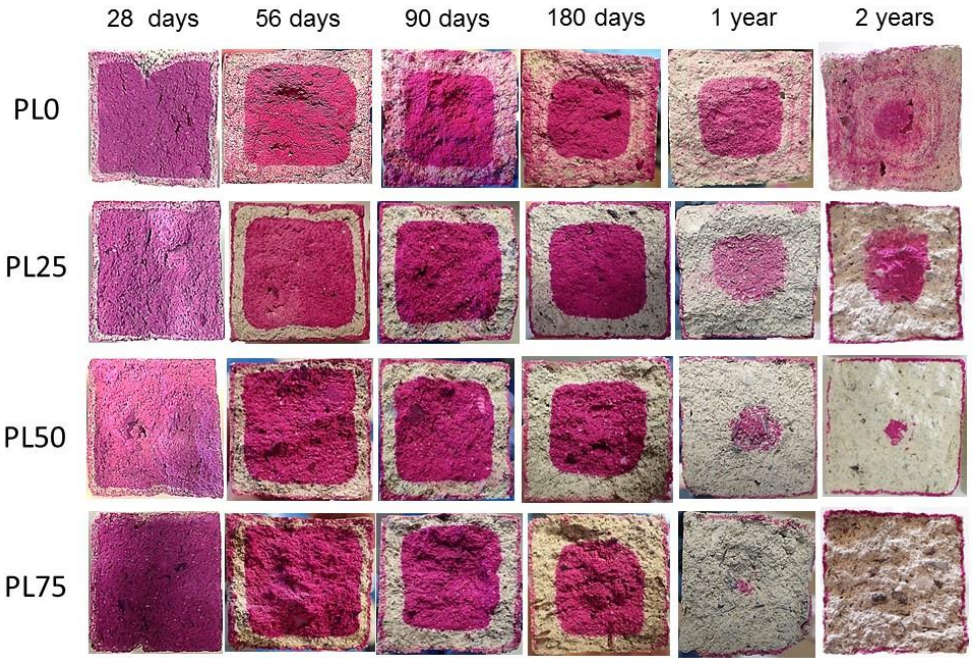

Figure 8. Carbonation front at 28, 56, 90, 180 days and, 1 and 2 years of age.

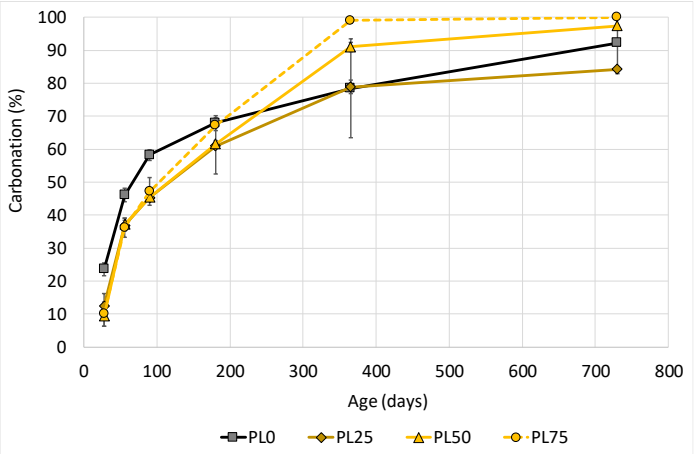

Figure 9. Rate of carbonation from 28 days to 2 years of age.

4.5 Compressive strength and ultrasonic wave propagation

Mechanical strength increases with ageing in all mortars due to the carbonation process. Results at 7, 28, 90 and 180 days and 1 and 2 years are presented in Figure 10.

Unlike cement based mortars, lime based mortars need a long time to develop their strength, at 365 days the compressive strength is about twice the value obtained at 28 days. All mussel shell mortars show compressive strength values higher than 1.5 MPa at 90 days, higher than 2 MPa at 180 days and around 3 MPa at 365 days. These values are similar to those shown in the literature. Lanas and Alvarez [36], with a binder to aggregate ratio of 1:3, obtained values below 2 MPa at 90 and 180 days and below 3 MPa at 1 year of age. In the work of Faria and Martins [37], compressive strength (at 60 and 120 days) of lime putty and hydrated lime mortars, with similar dosages to those used in this work, was lower than the strength of mussel shell mortars at all ages. Compressive strength values at 180 days, 1 year and 2 years of age presented in the work of Stefanidou and Papayianni [38] were also slightly lower than those obtained using mussel shell mortars.

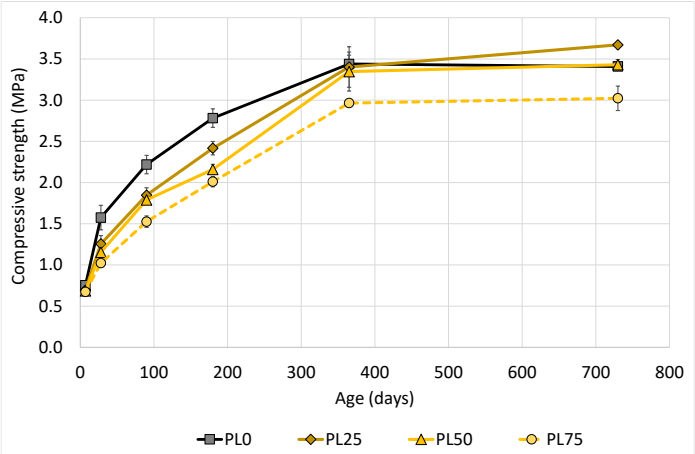

Figure 10. Compressive strength at 7, 28, 90, 180, 365 days and 2 years (MPa).

Compressive strength is controlled by porosity and carbonation. It is clear that porosity reduces the mortars' mechanical strength. However, as discussed in the previous section, it enhances the carbonation rate, leading mussel mortars to present a higher carbonation area than reference mortars at older ages, which could result in strength improvements.

As previously analysed (pore structure and microstructure), mussel aggregate particles are flaky and smooth; these characteristics weaken the bond between the air lime matrix and mussel aggregate leading to the production of a high volume of large pores in the ITZs of mussel shell mortars. Additionally, all mussel mortars presented a matrix phase with small drying cracks. All of these issues have a significant negative influence on the mortar's mechanical performance.

These two opposite effects lead mussel mortars to present compressive strength values lower than those obtained with the reference mortar at all ages. Therefore, the high carbonation area does not compensate for the effect of high porosity and the weak ITZ of mussel mortars. Furthermore, the curves that describe compressive strength evolution (Figure 10) show lower slope values in mussel mortars than in the reference mortar at younger ages. This trend changes at older ages, (especially 180 and 365) where, during this period, the slope of the curve is higher in mussel shell mortars than in the reference mortar.

This effect reflects the different carbonation rate at young and old ages, confirming that there is a direct relationship between carbonation and the hardening and mechanical strength of air lime mortars (Figure 11).

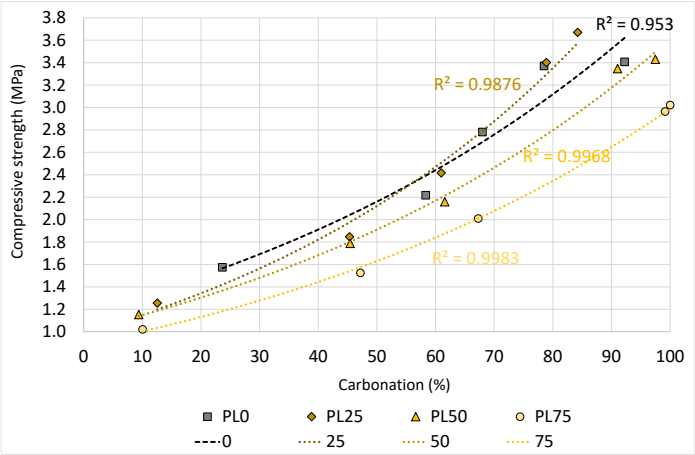

Figure 11. Carbonation vs compressive strength (at 28, 90, 180, 365 and 730 days).

Results of the ultrasonic test were measured at 7, 28, 180 days and 1 and 2 years (Figure 12). The ultrasound speed propagation (Vp) values obtained from all mortars are similar to those presented by other authors [23,39,40] working with similar dosages of lime-based mortars. All values are in the range of 1.1-1.5 km/s at 28 days, 1.8-2.1 km/s at 180 days and 1.9-2.2 km/s at 2 years.

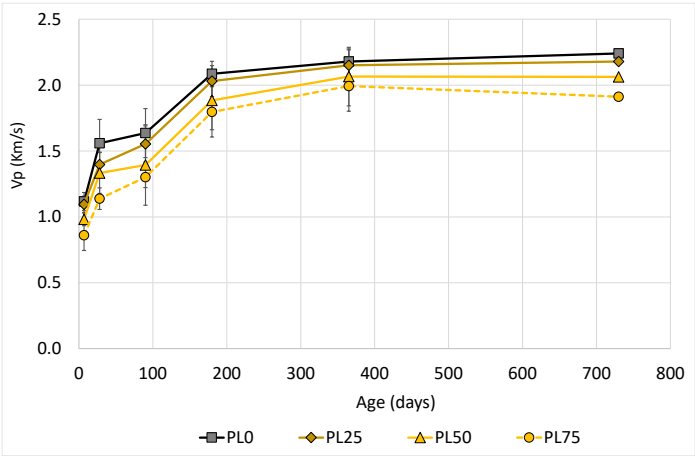

Figure 12. Ultrasonic wave propagation (Vp) from 7 days up to 2 years of age (at 7, 28, 90, 180, 365 and 730 days).

Ultrasonic wave propagation of lime mortars is highly influenced by hardening (i.e. the carbonation process that affects a mortar's porosity) and also by the mineralogy, grading and dosage of the aggregates used [23,39,40]. Arizzi et al. [23] stated that aggregate and water content have a direct relationship with wave attenuation in mortars. An increase in any of these leads to an increase in the values of the attenuation parameter. As in this work, the water content is the same in all mortars, and the differences can be attributed to the different morphology of the aggregates and differences in the carbonation rate.

The carbonation process produces an increase in mechanical strength and compactness, so a direct comparison of ultrasonic wave propagation and compressive strength of lime mortars can be done. As seen in **¡Error! No se encuentra el origen de la referencia.**, all the mortars show the same trend over time and as the compressive strength increases there is an improvement in wave propagation. However, when mortars with the same compressive strength value are compared, the Vp is lower in mortars with a higher replacement percentage of mussel shell aggregate. This means that mussel shell aggregate microstructure and probably its shape, may be causing the wave attenuation.

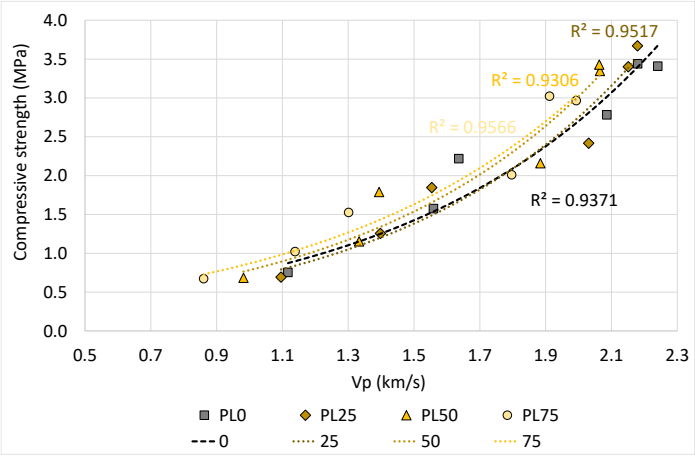

Figure 13. Ultrasonic wave propagation vs compressive strength. (con 180d)

5 Conclusions

The evolution over time of mussel shell coating mortars with lime putty was analysed. Three substitution percentages (25%, 50% and 75%) of conventional aggregate with mussel shell aggregate were used. The main conclusions drawn are as follows:

- Density results show two phases in all mortars. Firstly, where density decreases due to the loss of water and secondly, where it increases due to the carbonation process. The second phase is faster in mussel shell mortars than in baseline mortars.
- The porosity evolution of all mortars decreases with ageing in agreement with the carbonation process which hardens lime mortars and involves an increase in the solid volume.
- Analysis of the pore size distribution shows two peaks that decrease over time due to carbonation, with a higher decrease observed in mussel shell mortars. In the structural peak mussel shell mortars present a lower volume of pores than the reference mortar, due to the higher absorption of the mussel shell aggregates compared to limestone sand and the fact that mussel shell aggregate acts as a moisture retainer. Mussel shell mortars present a higher ITZ peak, and the range values of this peak is wider as the mussel shell content increases.
- In SEM images, PL75 shows a more disaggregated microstructure at all ages when compared to the baseline mortar. A lack of bond between mussel shell particles and lime paste can be seen at 28 days. Furthermore, at 1 year of age some small cracks are observed in mortars with a high replacement percentage, probably caused by the NaCl crystals. The organic matter content of mussels modifies the texture and microstructure of the crystals of calcium carbonate polymorphs at all ages.
- The carbonation rate in mortars with mussel shell displays two different trends. At young ages mussel shell reduces carbonation due to pore structure and organic matter content, this trend changes from 180 days onwards where the more mussel shell content the higher the carbonated area observed.

- Mussel aggregate particles are flaky and smooth; these characteristics weaken the bond between the air lime matrix and mussel aggregate producing a high volume of large pores in the ITZs of mussel shell mortars. However, the high carbonation area does not compensate for the effect of the high porosity and weak ITZ of mussel mortars, leading mussel mortars to present compressive strength values lower than those obtained with the reference mortar at all ages.
- Ultrasonic wave propagation in lime mortars is influenced by the carbonation rate and aggregate morphology. Mussel shell aggregate causes wave attenuation.

6 Acknowledgement

This work has been carried out within the framework of the following projects: “Assessment of Galician bivalve shell in the construction sector”; Code 00064742 / ITC-20133094, funded by CDTI under the FEDER-Innterconecta Program, and co-financed with European Union ERDF funds and “Sustainable High Performance Self Compacting Concrete using low clinker cement and internal curing and self healing agents”; Code BIA2017-85657-R funded by MINECO.

7 References

[1] R. Veiga, Air lime mortars: What else do we need to know to apply them in conservation and rehabilitation interventions? A review, Constr. Build. Mater. 157 (2017) 132–140. doi:10.1016/j.conbuildmat.2017.09.080.

[2] A. Arizzi, J. Martínez Martínez, G. Cultrone, D. Benavente, Mechanical Evolution of Lime Mortars during the Carbonation Process, Key Eng. Mater. 465 (2011) 483–486. doi:10.4028/www.scientific.net/KEM.465.483.

[3] W.. Tasong, C.. Lynsdale, J.. Cripps, Aggregate-cement paste interface. ii: influence of aggregate physical properties, Cem. Concr. Res. 28 (1998) 1453–1465. doi:10.1016/S0008-8846(98)00126-4.

[4] J.P. Gonçalves, L.M. Tavares, R.D. Toledo Filho, E.M.R. Fairbairn, E.R. Cunha, Comparison of natural and manufactured fine aggregates in cement mortars, Cem. Concr. Res. 37 (2007) 924–932. doi:10.1016/J.CEMCONRES.2007.03.009.

[5] M. Stefanidou, E. Anastasiou, K. Georgiadis Filikas, Recycled sand in lime-based mortars, Waste Manag. 34 (2014) 2595–2602. doi:10.1016/j.wasman.2014.09.005.

[6] C. Martínez-García, B. González-Fonteboa, D. Carro-López, F. Martínez-Abella, Impact of mussel shell aggregates on air lime mortars. Pore structure and carbonation, J. Clean. Prod. 215 (2019) 650–668. doi:10.1016/j.jclepro.2019.01.121.

[7] R. Walker, S. Pavia, R. Mitchell, Mechanical properties and durability of hemp-lime concretes, Constr. Build. Mater. 61 (2014) 340–348. doi:10.1016/j.conbuildmat.2014.02.065.

[8] R.S. J.I.Alvarez, J.M.Fernández, I.Navarro-Blasco, A.Duran, Microstructural consequences of nanosilica addition on aerial lime binding materials: Influence of different drying conditions, Mater. Charact. 80 (2013) 36–49. doi:https://doi.org/10.1016/j.matchar.2013.03.006.

[9] R. Alavéz-Ramírez, P. Montes-García, J. Martínez-Reyes, D.C. Altamirano-Juárez, Y. Gochi-Ponce, The use of sugarcane bagasse ash and lime to improve the durability and mechanical properties of compacted soil blocks, Constr. Build. Mater. 34 (2012) 296–305. doi:https://doi.org/10.1016/j.conbuildmat.2012.02.072.

[10] A. Izaguirre, J. Lanas, J.I. Álvarez, Behaviour of a starch as a viscosity modifier for aerial lime-based mortars, Carbohydr. Polym. 80 (2010) 222–228. doi:https://doi.org/10.1016/j.carbpol.2009.11.010.

[11] L. Falchi, E. Zendri, U. Müller, P. Fontana, The influence of water-repellent admixtures on the behaviour and the effectiveness of Portland limestone cement mortars, Cem. Concr. Compos. 59 (2015) 107–118. doi:10.1016/J.CEMCONCOMP.2015.02.004.

[12] G. Cultrone, E. Sebasti??n, M.O. Huertas, Forced and natural carbonation of lime-based mortars with and without additives: Mineralogical and textural changes, Cem. Concr. Res. 35 (2005)

2278–2289. doi:10.1016/j.cemconres.2004.12.012.

[13] G. Di Bella, V. Fiore, G. Galtieri, C. Borsellino, A. Valenza, Effects of natural fibres reinforcement in lime plasters (kenaf and sisal vs. Polypropylene), Constr. Build. Mater. 58 (2014) 159–165. doi:10.1016/j.conbuildmat.2014.02.026.

[14] L. Ventolà, M. Vendrell, P. Giraldez, L. Merino, Traditional organic additives improve lime mortars: New old materials for restoration and building natural stone fabrics, Constr. Build. Mater. 25 (2011) 3313–3318. doi:10.1016/J.CONBUILDMAT.2011.03.020.

[15] C. Nunes, P. Mácová, D. Frankeová, R. Ševčík, A. Viani, Influence of linseed oil on the microstructure and composition of lime and lime-metakaolin pastes after a long curing time, Constr. Build. Mater. 189 (2018) 787–796. doi:10.1016/J.CONBUILDMAT.2018.09.054.

[16] P. Pahlavan, S. Manzi, A. Sansonetti, M.C. Bignozzi, Valorization of organic additions in restorative lime mortars: Spent cooking oil and albumen, Constr. Build. Mater. 181 (2018) 650–658. doi:10.1016/j.conbuildmat.2018.06.089.

[17] K.A. Gour, R. Ramadoss, T. Selvaraj, Revamping the traditional air lime mortar using the natural polymer – Areca nut for restoration application, Constr. Build. Mater. 164 (2018) 255–264. doi:10.1016/j.conbuildmat.2017.12.056.

[18] I. Centauro, E. Cantisani, C. Grandin, A. Salvini, S. Vettori, The influence of natural organic materials on the properties of traditional lime-based mortars, Int. J. Archit. Herit. 11 (2017) 670–684. doi:10.1080/15583058.2017.1287978.

[19] P. Zhao, M.D. Jackson, Y. Zhang, G. Li, P.J.M. Monteiro, L. Yang, Material characteristics of ancient Chinese lime binder and experimental reproductions with organic admixtures, Constr. Build. Mater. 84 (2015) 477–488. doi:https://doi.org/10.1016/j.conbuildmat.2015.03.065.

[20] K. Zhang, A. Grimoldi, L. Rampazzi, A. Sansonetti, C. Corti, Contribution of thermal analysis in the characterization of lime-based mortars with oxblood addition, Thermochim. Acta. 678 (2019) 178303. doi:https://doi.org/10.1016/j.tca.2019.178303.

[21] C. Martínez-García, B. González-Fonteboa, F. Martínez-Abella, D. Carro- López, Performance of mussel shell as aggregate in plain concrete, Constr. Build. Mater. 139 (2017) 570–583. doi:10.1016/j.conbuildmat.2016.09.091.

[22] L. Génio, S. Kiel, M.R. Cunha, J. Grahame, C.T.S. Little, Shell microstructures of mussels (Bivalvia: Mytilidae: Bathymodiolinae) from deep-sea chemosynthetic sites: Do they have a phylogenetic significance?, Deep. Res. Part I Oceanogr. Res. Pap. 64 (2012). doi:10.1016/j.dsr.2012.02.002.

[23] A. Arizzi, J. Martínez-Martínez, G. Cultrone, Ultrasonic wave propagation through lime mortars: an alternative and non-destructive tool for textural characterization, Mater. Struct. 46 (2013) 1321–1335. doi:10.1617/s11527-012-9976-1.

[24] C. Martínez-García, B. González-Fonteboa, D. Carro-López, F. Martínez-Abella, Design and properties of cement coating with mussel shell fine aggregate, Constr. Build. Mater. 215 (2019) 494–507. doi:10.1016/j.conbuildmat.2019.04.211.

[25] M. Arandigoyen, J.L.P. Bernal, M.A.B. López, J.I. Alvarez, Lime-pastes with different kneading water: Pore structure and capillary porosity, Appl. Surf. Sci. 252 (2005) 1449–1459. doi:10.1016/j.apsusc.2005.02.145.

[26] Ö. Cizer, K. Van Balen, J. Elsen, D. Van Gemert, Crystal morphology of precipitated calcite crystals from accelerated carbonation of lime binders, Proc. ACEME08, 2nd Int. Conf. Accel. Carbonation Environ. Mater. Eng. (2008).

[27] Ö. Cizer, C. Rodriguez-Navarro, E. Ruiz-Agudo, J. Elsen, D. Van Gemert, K. Van Balen, Phase and morphology evolution of calcium carbonate precipitated by carbonation of hydrated lime, J. Mater. Sci. 47 (2012) 6151–6165. doi:10.1007/s10853-012-6535-7.

[28] Ö. Cizer, K. Van Balen, J. Elsen, D. Van Gemert, Real-time investigation of reaction rate and mineral phase modifications of lime carbonation, Constr. Build. Mater. 35 (2012) 741–751. doi:10.1016/j.conbuildmat.2012.04.036.

[29] H. Liu, Y. Zhao, C. Peng, S. Song, A. López–Valdivieso, Lime mortars – The role of carboxymethyl

cellulose on the crystallization of calcium carbonate, Constr. Build. Mater. 168 (2018) 169–177. doi:https://doi.org/10.1016/j.conbuildmat.2018.02.119.

[30] D. Ergenç, R. Fort, Accelerating carbonation in lime-based mortar in high CO2 environments, Constr. Build. Mater. 188 (2018) 314–325. doi:https://doi.org/10.1016/j.conbuildmat.2018.08.125.

[31] L.S. Gomez-Villalba, P. López-Arce, M.A. De Buergo, R. Fort, Structural stability of a colloidal solution of Ca(OH) 2nanocrystals exposed to high relative humidity conditions, Appl. Phys. A Mater. Sci. Process. 104 (2011) 1249–1254. doi:10.1007/s00339-011-6457-2.

[32] S.J.C. Granneman, B. Lubelli, R.P.J. Van Hees, Characterization of lime mortar additivated with crystallization modifiers, Int. J. Archit. Herit. 12 (2018) 849–858. doi:10.1080/15583058.2017.1422570.

[33] M. Thomson, J. Lindqvist, J. Elsen, C. Groot, Chapter 2.5 Characterisation: Porosity of mortars, in: 2007: p. 75.

[34] R.M. Lawrence, T.J. Mays, S.P. Rigby, P. Walker, D. D'Ayala, Effects of carbonation on the pore structure of non-hydraulic lime mortars, Cem. Concr. Res. 37 (2007) 1059–1069. doi:10.1016/j.cemconres.2007.04.011.

[35] K. Van Balen, Carbonation reaction of lime, kinetics at ambient temperature, Cem. Concr. Res. 35 (2005) 647–657. doi:10.1016/j.cemconres.2004.06.020.

[36] J. Lanas, J.I. Alvarez, Masonry repair lime-based mortars: Factors affecting the mechanical behavior, Cem. Concr. Res. 33 (2003) 1867–1876. doi:10.1016/S0008-8846(03)00210-2.

[37] P. Faria, A. Martins, Influence of Air Lime type and Curing Conditions on Lime and Lime-Metakaolin Mortars, in: J. Freitas, V.; Delgado (Ed.), Durab. Build. Mater. Components. Build. Pahology Rehabil., Vol 3, Springer, Berlin, Heidelberg, 2013: pp. 105–126. doi:10.1007/978-3-642-37475-3_5.

[38] M. Stefanidou, I. Papayianni, The role of aggregates on the structure and properties of lime mortars, Cem. Concr. Compos. 27 (2005) 914–919. doi:10.1016/J.CEMCONCOMP.2005.05.001.

[39] O. Cazalla, C. Rodriguez-Navarro, E. Sebastian, G. Cultrone, M.J. Torre, Aging of Lime Putty: Effects on Traditional Lime Mortar Carbonation, J. Am. Ceram. Soc. 83 (2004) 1070–1076. doi:10.1111/j.1151-2916.2000.tb01332.x.

[40] A. Arizzi, G. Cultrone, The influence of aggregate texture, morphology and grading on the carbonation of non-hydraulic (aerial) lime-based mortars, Q. J. Eng. Geol. Hydrogeol. 46 (2013) 507–520. doi:10.1144/qjegh2012-017.